Microchim Acta (2015) 182:1701–1708
DOI 10.1007/s00604-015-1501-0

ORIGINAL PAPER

Nonenzymatic amperometric sensing of glucose using a glassy carbon electrode modified with a nanocomposite consisting of reduced graphene oxide decorated with Cu_2O nanoclusters

Li-Ping Mei[1] · Pei Song[1] · Jiu-Ju Feng[1] · Jia-Hui Shen[1] · Wei Wang[1] · Ai-Jun Wang[1] · Xuexiang Weng[1]

Received: 13 January 2015 / Accepted: 13 April 2015 / Published online: 28 April 2015

Abstract We describe a simple solvothermal method for preparation of reduced graphene oxide nanosheets decorated with uniform Cu_2O nanoclusters by using poly(vinyl pyrrolidone)-poly(methacrylamide)-poly(vinyl imidazole) triblock co-polymer as a shape-directing agent and *L*-glutamic acid as a reducing agent. The resulting nanocomposite was deposited on a glassy carbon electrode where it displays improved electrocatalytic activity toward glucose oxidation in 0.5 M NaOH. This observation was exploited to construct a nonenzymatic amperometric sensor for glucose. It has a detection limit as low as 1.0 μM, high sensitivity (23.058 μA mM^{-1}), and a dynamic (analytical) range that extends from 5.0 to 9595 μM at a working potential of 600 mV (vs. SCE).

Keywords Reduced graphene oxide · Nanoclusters · Triblock copolymer · Glucose · Electrocatalysis

Introduction

A variety of noble metal nanostructures with desired physical and/or chemical properties has been prepared [1], but their high price and rare storage seriously confine their commercial applications. Therefore, it is essential to search for low-cost and plentiful metals (e.g., Ni, Cu, Co, and Fe) as alternatives.

Cu_2O is one of the most investigated semiconductors and has wide applications in CO oxidation, biosensors, solar energy conversion, and photocatalysis [2]. Its catalytic properties are tightly correlated with the respective structural features, size, and morphology [3]. As a result, it is highly desired to prepare novel Cu_2O nanocatalysts with fine-controlled structure, dimension, and shape [4]. Accordingly, many shape-controlled Cu_2O nanostructures have been prepared, including cages [5], cubes [6], and spheres [7].

Many supports have been introduced to endow the above catalysts with well distribution, especially graphene oxide (GO) nanosheets [7] or reduced graphene oxide (r-GO) [7], owing to their enlarged surface area, high electrical conductivity, better chemical stability, and strong adhesion to the catalysts [8]. To date, many nanocomposites, especially metal oxide-graphenes, have been synthesized, including Cu_2O-graphene [9], NiO-graphene [10], TiO_2-graphene [11], and MnO_2-graphene [12].

Enzyme-based electrochemical biosensors display high sensitivity and selectivity [13]. Nevertheless, they suffer from poor stability and reproducibility. Alternatively, non-enzymatic sensors possess better durability and stability against external environment toward glucose oxidation [14]. For example, Zhou et al. fabricated monodisperse porous Cu_2O/r-GO, which showed excellent catalytic activity and good selectivity for glucose detection [15]. In another example, Gao's group prepared mesocrystalline Cu_2O hollow nanocubes for construction of glucose sensors [14]. However, their relatively higher detection limit and narrow linear range are unsatisfied during accurately monitoring glucose.

Electronic supplementary material The online version of this article (doi:10.1007/s00604-015-1501-0) contains supplementary material, which is available to authorized users.

✉ Ai-Jun Wang
ajwang@zjnu.cn

✉ Xuexiang Weng
xuexian@zjnu.cn

[1] College of Geography and Environmental Science, College of Chemistry and Life Science, Zhejiang Normal University, Jinhua 321004, China

Polymers have strong interactions and sometimes form coordination complexes with nanocrystals, and thereby influence the growth kinetics of the nanocrystals as capping agents and shape-directing agents [16]. A variety of polymers (e.g., cationic, anionic and nonionic polymers) has been used for shape-controlled synthesis of nanocrystals [17]. Polyvinylpyrrolidone (PVP) is the most frequently used nonionic polymer in this field [18]. Copolymers, containing two or more different monomers, have more functional properties [19]. For example, poly(ethylene glycol)-block-poly(propylene glycol)-block-poly(ethylene glycol) Pluronic® P123 was used as a shape-directing agent for shape-controlled synthesis of mesoporous silica [20].

Herein, a facile solvothermal method is described for synthesis of uniform Cu_2O nanoclusters on r-GO (denoted as Cu_2O NCs/r-GO), using poly(vinyl pyrrolidone)-poly(methacrylamide)-poly(vinyl imidazole) triblock copolymer (Fig. S1, Electronic Supplementary Material, ESM) and *L*-glutamic acid as a shape-directing agent and a reducing agent. The catalytic performance of Cu_2O NCs/r-GO was investigated through the fabrication of a non-enzymatic glucose sensor.

Experimental

Reagents and materials

Copper(II) nitrate trihydrate, sodium hydroxide, and glucose were purchased from Shanghai Sigma-Aldrich (Shanghai, China, www.sigmaaldrich.com). Poly(vinyl pyrrolidone)-poly(methacrylamide)-poly(vinyl imidazole) triblock copolymer (Luviset^R Clear), graphite powder (99.95 %, 8000 mesh), *L*-glutamic acid, ascorbic acid (AA), dopamine (DA), uric acid (UA), lactic acid, glutaric acid, acetaminophen, and $NaBH_4$ were bought from Shanghai Aladdin Chemical Reagent Company (Shanghai, China, www.chemicalbook.com). The other chemicals were of analytical grade and used without further purification. Double distilled-water was used to prepare all of the aqueous solutions throughout the whole experiments.

Preparation of Cu_2O NCs/r-GO and of Cu_2O nanoparticles

Typically, GO was prepared from natural graphite powder by a modified Hummers' method, and experimental details are given in the previous work [21].

For typical preparation of Cu_2O NCs/r-GO, 0.5 g of poly(-vinyl pyrrolidone)-poly(methacrylamide)-poly(vinyl imidazole) triblock copolymer was dissolved into 15 mL of ethanol under stirring. Then, 5 mL of GO (1 mg mL^{-1}), 0.121 g of $Cu(NO_3)_2 \cdot 3H_2O$, and 0.3 g of *L*-glutamic acid were put into the mixed solution, respectively. After homogeneously stirring, the mixed solution was transferred into a Teflon lined stainless steel autoclave (25 mL), heated at 160 °C for 6 h, and cooled to 25 °C in air. The final black precipitates were collected by centrifugation, thoroughly washed with water and ethanol for several times, and dried in vacuum at 60 °C for further characterization.

Similarly, Cu_2O nanoparticles were fabricated without GO for comparison, and pure r-GO were obtained by reducing GO with $NaBH_4$, while other conditions were kept unchanged.

Characterization

The morphology of the samples was characterized by transmission electron microscopy (TEM) and high-resolution transmission electron microscopy (HRTEM), which were performed on a JEM-2100 F transmission electron microscope (www.jeol.co.jp/en.com) equipped with the selective area electron diffraction (SAED). The crystal structures were determined by X-ray diffraction (XRD, Rigaku Dmax-2000 diffractometer) using Cu-Kα radiation (Bruker Co., Germany, www.rigaku.com). X-ray photoelectron spectra (XPS) were recorded on a Thermo Scientific Escalab 250 XPS spectrometer (www.pharmaceuticalonline.com) with Al Kα X-ray radiation (1486.6 eV). Fourier transform infrared (FT-IR) analysis was performed on a Nicolet NEXUS670 spectrometer (http://web.ysu.edu/gen/stem). Raman spectra were acquired on a micro-Raman system (Renishaw RM1000 spectrometer) with an excitation wavelength of 633 nm (www.antpedia.com). Thermogravimetric analysis (TGA) was conducted with a simultaneous thermo-gravimetric analyzer (Netzsch, STA 449C, www.brain-power.com). The samples were heated in air from 25 to 800 °C at a heating rate of 10 °C min^{-1}.

Electrochemical measurements

The electrochemical measurements were conducted on a CHI660D electrochemical workstation (Chenhua Instruments Co., Shanghai, China, www.chinstruments.com), and performed with a conventional three-electrode system, including a platinum wire as the counter electrode, a saturated calomel electrode (SCE, saturated KCl) as the reference electrode, and a bare or modified glassy carbon electrode (GCE, 3.0 mm in diameter) as the working electrode.

For typical construction of Cu_2O NCs/r-GO modified electrode (Cu_2O NCs/r-GO/GCE), 2.0 mg of Cu_2O NCs/r-GO was dispersed into 1.0 mL water under ultrasonication to form a homogeneous suspension. Next, 8 μL of the suspension was casted on the clean GCE and dried naturally, followed by casting another layer of Nafion (0.05 wt %) with the volume of 5 μL to fix the deposit on the electrode surface. For comparison, individual r-GO and Cu_2O modified electrodes

were prepared in a similar way, denoted as r-GO/GCE and Cu_2O NCs/GCE, respectively.

The electrocatalytic activity of the above catalysts modified electrodes was determined by linear sweep voltammetry toward glucose oxidation in 0.5 M NaOH at a scan rate of 50 mV s^{-1}. The stability of Cu_2O NCs/r-GO/GCE was examined by amperometry at an applied potential of 600 mV in 0.5 M NaOH. The electrochemical experiments were carried out at 25 °C, if not stated otherwise.

Results and discussion

Characterization

As seen from TEM images (Fig. 1a and b), the product mainly consists of numerous well-defined nanoclusters across the whole section, without any agglomerating, which are uniformly dispersed on r-GO. The nanoclusters have a very narrow size distribution from 1.2 to 3.9 nm (Fig. 1d), with the average size of 2.6 nm. Their polycrystalline nature is demonstrated by the corresponding SAED pattern (inset in Fig. 1b). HRTEM image (Fig. 1c) shows the well-defined lattice fringes with the inter-planar spacing of *ca*. 0.19 nm, which is in good accordance with the (200) crystal planes of Cu_2O.

It is known that surfactants have great effects on the morphology and size of nanocrystals [16, 17]. As expected, only some irregular, agglomerated, and large Cu_2O particles (Fig. 2a, b) are obtained without or using smaller amount of the triblock copolymer (0.1 %). When the amounts of the triblock copolymer are 0.5 % (Fig. 2c) and 1.0 % (Fig. 2d), numerous Cu_2O nanoparticles with decreased sizes are observed on r-GO. These results indicate that the amounts of the triblock copolymer played the essential role in controlling the morphology and size of Cu_2O NCs.

Fig. S2 (ESM) provides the XRD pattern of Cu_2O NCs/r-GO, using r-GO as a reference. Clearly, there are four representative diffraction peaks emerged at 36.5, 42.6, 61.5, and 73.6°, which are well assigned to the (111), (200), (220), and (311) planes of the face-centered cubic (fcc) structure of Cu_2O [22, 23]. These values are matched well with the Joint Committee Powder Diffraction Standard of pure Cu_2O (JCPDS No. 05–0667). The corresponding (111) diffraction peak is stronger and sharper than those of the other planes, showing the preferential growth of Cu_2O NCs along the (111) directions [15]. Furthermore, there are no any other peaks of impurities (e.g., CuO and Cu) emerged, indicating high purity of Cu_2O NCs. In addition, a new broad peak is observed at 2θ =19.4° for Cu_2O NCs/r-GO (Fig. S2, ESM, curve a), which is consistent with that of r-GO (Fig. S2, ESM, curve b, 2θ=20.9°), suggesting the efficient removal of oxygen-containing functional groups and well dispersion of Cu_2O NCs on r-GO [24].

The composition and surface states of Cu_2O NCs/r-GO were examined by XPS measurements. The XPS survey spectrum (Fig. 3a) demonstrates the coexistence of Cu, O, N, and C elements in Cu_2O NCs/r-GO. As for high-resolution Cu XPS spectrum (Fig. 3b), there are two peaks detected at 933.7 and 953.8 eV, which are assigned to the binding energies of Cu $2p_{3/2}$ and Cu $2p_{1/2}$ of Cu(I) [25, 26], respectively. A

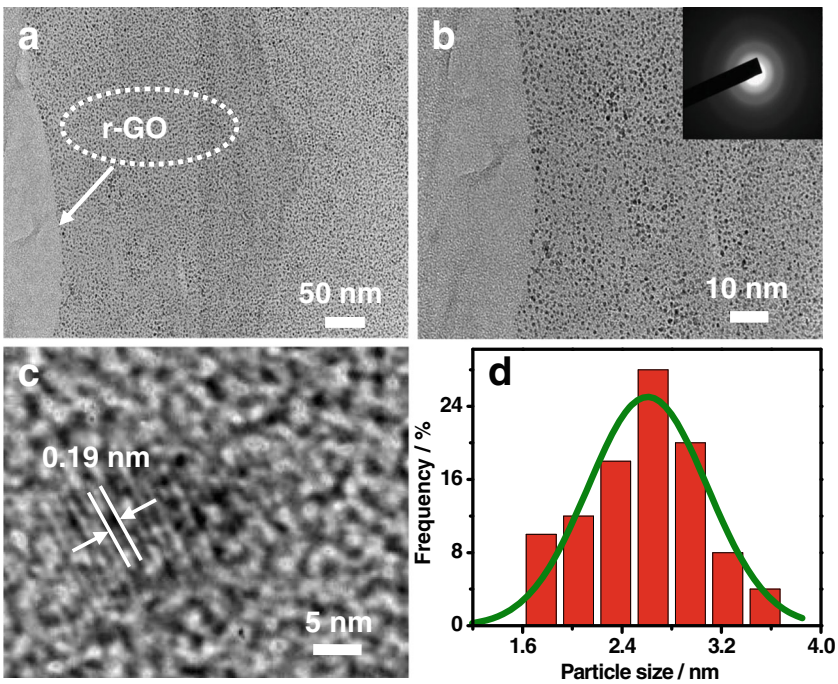

Fig. 1 **a**, **b** TEM, and (**c**) HRTEM images of Cu_2O NCs/r-GO using 2.5 % triblock copolymer. **d** The corresponding size-distribution histograms. Inset in B shows the corresponding SAED pattern

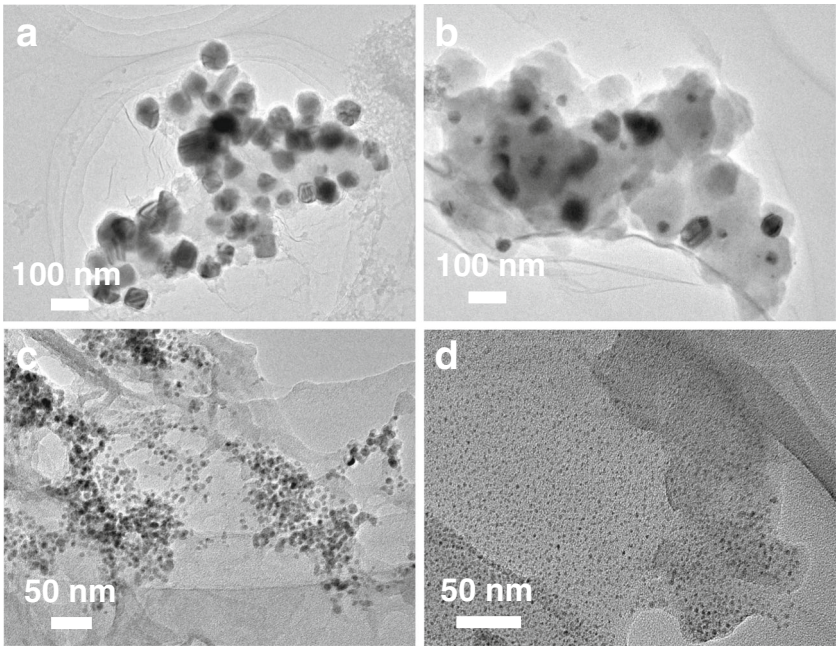

Fig. 2 TEM images of Cu_2O nanoparticles obtained with different concentrations of the triblock copolymer **a** 0 %, **b** 0.1 %, **c** 0.5 %, and **d** 1.0 %

weak peak shows up at 943.7 eV, suggesting that there is a very minimal amount of Cu(II) present in this system, which may be derived from the un-reacted precursor of $Cu(NO_3)_2$ [27]. By measuring their relative intensities, Cu(I) is the predominant species, revealing the formation of Cu_2O NCs.

High-resolution C 1 s XPS spectrum of Cu_2O NCs/r-GO (Fig. 3c) can be well fitted into four peaks at 284.70, 285.70, 287.58 eV, and 288.67 eV, which are attributed to the C-C (sp^2), C-O, C = O, and O-C = O groups, respectively [28]. Particularly, the peaks related to the oxygen functionalities are much weaker in comparison with those of GO (Fig. 3d),

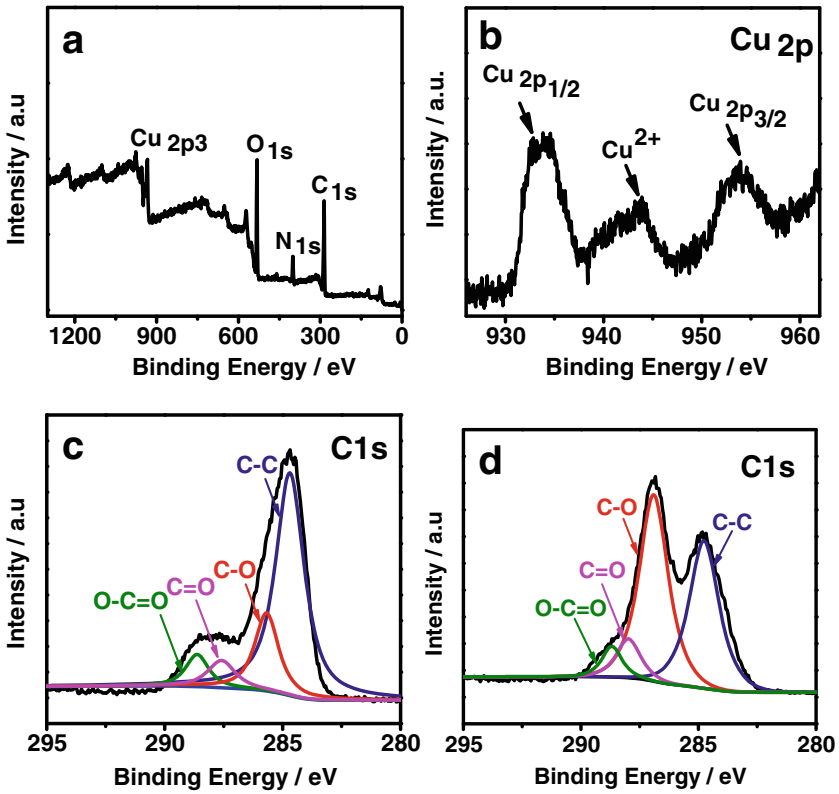

Fig. 3 **a** Survey, high-resolution **b** Cu 2p, and C 1 s XPS spectra of **c** Cu_2O NCs/r-GO and **d** GO, respectively

showing the formation of r-GO under hydrothermal conditions. This assumption is strongly supported by FT-IR spectra of Cu_2O NCs/r-GO (Fig. 4A). Notably, the peak intensities at 1046 cm^{-1} (O–H) and 1730 cm^{-1} (C = O) are greatly decreased for Cu_2O NCs/r-GO (curve a) as compared to those of GO (curve b).

Similarly, Raman spectra (Fig. 4B) display two characteristic peaks at 1362 and 1608 cm^{-1} for the *D* and *G* bands in Cu_2O NCs/r-GO (curve a) and GO (curve b), respectively. The integral area ratio of the two bands (denoted as I_D/I_G) is 1.5 for Cu_2O NCs/r-GO, which is larger than that of GO (0.82), indicating the efficient formation of r-GO [29].

TGA analysis was performed to test the thermal stability and estimate the metal loading of Cu_2O NCs/r-GO (Fig. S3, ESM). After heating from 25 to 800 °C, there is no weight left for GO because of the evaporation of water molecules, the removal of some oxygen-containing functional groups, and the decomposition of the carbon skeleton groups [30]. However, Cu_2O NCs/r-GO exhibit much lower mass loss and faster achievement of the thermal plateau under the identical conditions, manifesting their better thermal stability and efficient reduction of GO to r-GO [31]. Additionally, the mass loading of Cu_2O is 30.7 wt. %.

Electrochemical properties of Cu_2O NCs/r-GO/GCE

Firstly, Cu_2O NCs/r-GO modified electrode was constructed to examine their electrocatalytic properties, using GCE and pure r-GO/GCE as referenced electrodes. Electrochemical impedance spectroscopy was employed to investigate the electrical conductivity of the nanocomposites to study the synergistic effects between r-GO and Cu_2O. Figure 5 shows Nyquist plots obtained on GCE (curve a), r-GO/GCE (curve b), and Cu_2O NCs/r-GO/GCE (curve c) in 0.1 M KCl containing 5.0 mM $[Fe(CN)_6]^{3-/4-}$(1:1) solutions. The diameter of a semicircle of Cu_2O NCs/r-GO modified electrode in high-frequency zone is larger than those of r-GO/GCE or bare GCE under the identical conditions. It means the larger

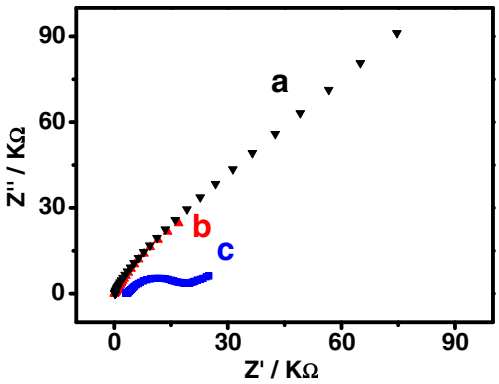

Fig. 5 EIS of GCE (*curve a*), r-GO/GCE (*curve b*), Cu_2O NCs/r-GO/GCE (*curve c*), and Cu_2O/GCE (*curve d*) in 0.1 M KCl containing 5.0 mmol L^{-1} $[Fe(CN)_6]^{3-/4-}$ solutions. Frequency range: 0.01 to 1×10^5 Hz

resistance for electron transfer on Cu_2O NCs/r-GO modified electrode as compared to those of the other two cases. This is ascribed to the fact that the decorated Cu_2O NCs as a semiconductor increase the resistance in Cu_2O NCs/r-GO as contrast to that of r-GO, reflecting the decreased conductivity of Cu_2O NCs/r-GO in the present work.

Herein, a non-enzymatic glucose sensor was constructed to investigate the electrocatalytic activity of Cu_2O NCs/r-GO (Fig. 6A, curve a) in 0.5 M NaOH containing 5.0 mM glucose, using individual r-GO (curve b) and Cu_2O NCs (curve c) as references. There is almost no anodic current observed at bare GCE. Clearly, Cu_2O NCs/r-GO modified electrode shows more negative onset potential and higher anodic currents in contrast to r-GO and Cu_2O NCs. It means the enhanced electrocatalytic performance of Cu_2O NCs/r-GO. This is attributed to the fact that the present redox pair of Cu(II)/Cu(III) leads to the easy oxidation of glucose in strongly alkaline media [32] and the fast electron transfer provided by r-GO [33].

Figure 6B illustrates a series of linear sweep voltammograms (LSVs) at Cu_2O NCs/r-GO modified electrode, displaying the enhanced anodic peak currents with glucose in the range of 10.0~35.0 mM. This observation confirms

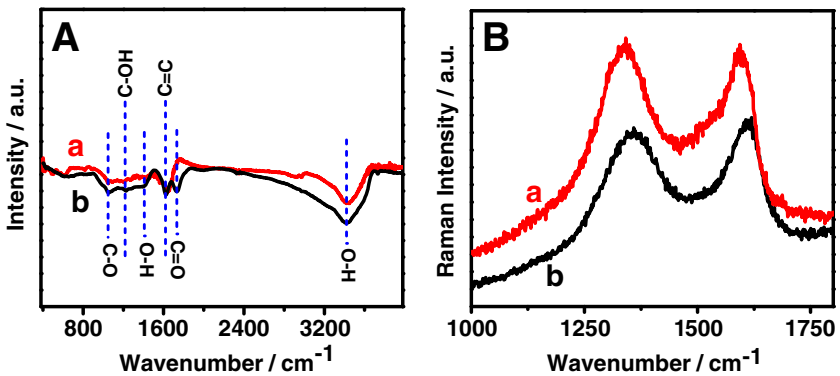

Fig. 4 **A** FT-IR and **B** Raman spectra of Cu_2O NCs/r-GO (*curve a*) and GO (*curve b*)

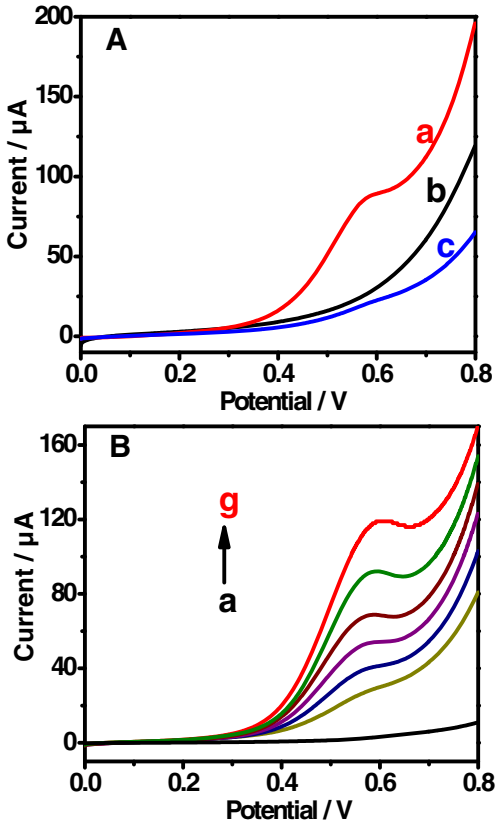

Fig. 6 **A** LSVs of Cu_2O NCs/r-GO (*curve a*), r-GO (*curve b*), and Cu_2O (*curve c*) modified electrodes in 0.5 M NaOH+5.0 mM glucose at a scan rate of 50 mV s^{-1}. **B** LSVs of Cu_2O NCs/r-GO modified electrode without (*curve a*) and with 10.0, 15.0, 20.0, 25.0, 30.0, and 35.0 mM glucose (*curve b–g*)

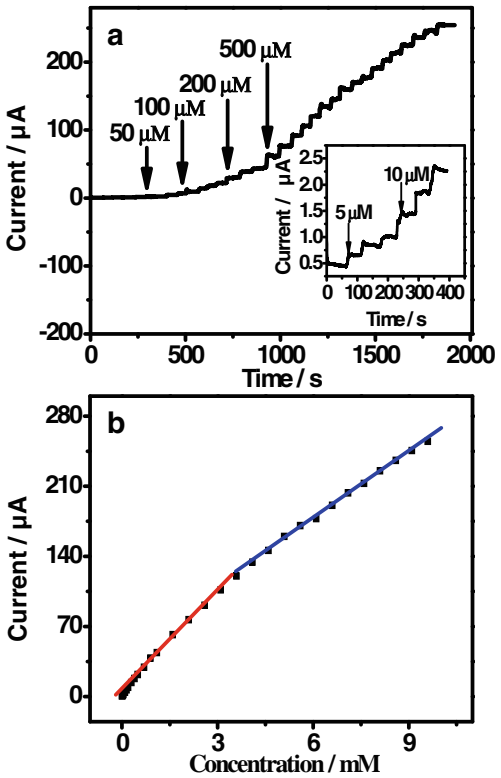

Fig. 7 **a** Amperometric i–t *curves* of Cu_2O NCs/r-GO modified electrode after successive addition of glucose to 0.5 M NaOH at 600 mV. **b** The corresponding calibration plot

the improved catalytic activity of Cu_2O NCs/r-GO for glucose oxidation. The maximum catalytic current is observed at the applied potential of 600 mV upon the addition of glucose, which is applied for amperometric determination of glucose.

Determination of glucose

Typical amperometric curves of Cu_2O NCs/r-GO modified electrode were recorded at 600 mV with successive addition of glucose into 0.5 M NaOH under constant stirring. As depicted in Fig. 7a, the amperometric response is less than 3 s, indicating rapid responses toward glucose, owing to the improved catalytic activity and fast electron transfer of Cu_2O NCs/r-GO with the electrode [4]. The plot shown in Fig. 7b does not fit a conventional linear equation in the whole concentration range. The linear regression equations are I (μA) =1.6301+37.5518C (R^2=0.9950) and I (μA) =37.7961+23.0580 C (R^2=0.9968) for determining glucose over the two linear concentration ranges of 0.005~2.095 mM and 2.595~9.595 mM, respectively. The detection limit is 1.0 μM at the signal-to-noise ratio (3S/N), which is much lower than most previously reported values [14, 15, 34–37]. It is notable that Cu_2O NCs/r-GO modified electrode displays the enhanced catalytic performance for glucose sensing in terms of sensitivity and the limits of detection (LOD), compared to those of Cu_2O-based materials previously reported (Table 1) [14, 15, 34–37].

Repeatability and stability

The repeatability of the sensor used in the measurement was obtained by recording the responses to 5.0 mM glucose in 0.5 M NaOH. The relative standard deviations (RSDs) were

Table 1 Comparison of Cu_2O-based sensors for glucose determination

Electrodes	Sensitivity (μA mM^{-1})	Linear range (mM)	LOD (mM)	Ref.
Porous Cu_2O nanosphere- r-GO	185	0.01~6.0	0.05	[14]
Hollow Cu_2O nanocubes	52.5	0.001~1.7	0.87	[15]
Cu-Cu_2O NWs	859.14	0.1~12	0.05	[33]
Cu/Cu_2O	33.63	0.22~10.89	0.05	[34]
Au/LDH-CNTs-G	141.22	0.01~6.1	0.001	[35]
MCo-CFs (M=Cu, Fe, Ni, and Mn)	35.82	0.02~11	0.001	[36]
Cu_2O NCs/r-GO	37.55; 23.06	0.005~2.095; 2.595~9.595	0.001	This work

calculated to be 2.0 % (n=5) for Cu_2O NCs/r-GO/GCE. Additionally, to evaluate the electrode-to-electrode reproducibility, they were independently prepared using the same way and revealed an acceptable reproducibility with low RSD values of 1.4 % (n=5). The stability of the sensor was examined by intermittently measuring the current responses to 5.0 mM glucose over a 35-day storage period (Fig. S4, ESM). The sensors were stored at 25 °C when not in use. The amperometric responses remained 95.2 % of their initial values after a storage period of 35 days, revealing long-term stability of the resulting sensor. The obtained sensor can be continuously detected without regenerating between each measurement.

Interference study and applications to human serum samples

To evaluate the selectivity of the sensor, potentially interfering biomolecules (i.e., UA, AA, and DA) were detected at Cu_2O NCs/r-GO modified electrodes, which usually coexist with glucose in real samples such as human blood. The interference study was investigated in the presence of 5.0 mM glucose. The criterion for interference was a relative error of less than±5 %. It was found that 500 folds of $CaCl_2$, $MgCl_2$, KCl, and NaCl, 50 folds of lactic acid and glutaric acid, 15 folds of UA and AA, 10 folds of DA and acetaminophen, and 5-fold concentrations of fructose and maltose had no interference in the determination of glucose. These results demonstrate good selectivity of the resulting sensor for glucose assay.

Glucose in human serum samples were determined by Cu_2O NCs/r-GO modified electrode at 600 mV. As shown in Table S1 (ESM), the as-obtained results are consistent with those determined by a hospital-used blood sugar instrument (Accu-Chek Performa), and the RSD values range from 1.23 to 2.37 %. These results display that the nonenzymatic sensor can be employed practically for routine analysis of glucose in real biological samples.

Conclusions

In summary, a facile solvothermal method was developed for preparation of Cu_2O NCs/r-GO, with the assistance of the triblock copolymer (Luviset^R Clear) and *L*-glutamic acid as a shape-directing agent and a reducing agent, respectively. The nanocomposites exhibit better catalytic activity than those of Cu_2O nanoparticles and r-GO toward glucose oxidation. The sensor has wide linear range (0.005 to 9.595 mM), high sensitivity (23.058 μA mM^{-1}), and selectivity. The improved performances of Cu_2O NCs/r-GO make it a promising candidate for the assay of glucose.

Acknowledgments This work was financially supported by National Natural Science Foundation of China (No. 21475118, 21175118 and 21275130), Zhejiang province university young academic leaders of academic climbing project (No. pd2013055), and Zhejiang normal university of undergraduate scientific and technological innovation project (New Talents Program, No. X201414 for LPM).

References

1. Guo S, Wang E (2011) Noble metal nanomaterials: Controllable synthesis and application in fuel cells and analytical sensors. Nano Today 6:240
2. Li X, Gao H, Murphy CJ, Gou L (2004) Nanoindentation of Cu_2O nanocubes. Nano Lett 4:1903
3. Wang J (2008) Electrochemical glucose biosensors. Chem Rev 108:814
4. Feng X-X, Guo C-F, Mao L-Y, Ning J-Q, Hu Y (2013) Facile growth of Cu_2O nanowires on reduced graphene sheets with high nonenzymatic electrocatalytic activity toward glucose. J Am Ceram Soc 97:811
5. Lu C-H, Qi L-M, Yang J-H, Wang X-Y, Zhang D-Y, Xie J-L, Ma J (2005) One-pot synthesis of octahedral Cu_2O nanocages via a catalytic solution route. Adv Mater 17:2562
6. Gou L, Murphy CJ (2003) Solution-phase synthesis of Cu_2O nanocubes. Nano Lett 3:231
7. Sinha B, Goswami T, Paul S, Misra A (2014) The impact of surface structure and band gap on the optoelectronic properties of Cu_2O nanoclusters of varying size and symmetry. RSC Adv 4:5092
8. Xia B-Y, Wang B, Wu H-B, Liu Z, Wang X, Lou X-W (2012) Sandwich-structured TiO_2–Pt–graphene ternary hybrid electrocatalysts with high efficiency and stability. J Mater Chem 22:16499
9. Jiang B-B, Wei X-W, Wu F-H, Wu K-L, Chen L, Yuan G-Z, Dong C, Ye Y (2014) A non-enzymatic hydrogen peroxide sensor based on a glassy carbon electrode modified with cuprous oxide and nitrogen-doped graphene in a nafion matrix. Microchim Acta 181:1463
10. Bajpai R, Roy S, Koratkar N, Misra D (2013) NiO nanoparticles deposited on graphene platelets as a cost-effective counter electrode in a dye sensitized solar cell. Carbon 56:56
11. Zhang Z-Y, Xiao F, Guo Y-L, Wang S, Liu Y-Q (2013) One-pot self-assembled three-dimensional TiO_2-graphene hydrogel with improved adsorption capacities and photocatalytic and electrochemical activities. ACS Appl Mater Interfaces 5:2227
12. Peng L, Peng X, Liu B, Wu C, Xie Y, Yu G (2013) Ultrathin two-dimensional MnO_2/graphene hybrid nanostructures for high-performance, flexible planar supercapacitors. Nano Lett 13:2151
13. Bhakta SA, Evans E, Benavidez TE, Garcia CD (2015) Protein adsorption onto nanomaterials for the development of biosensors and analytical devices: a review. Anal Chim Acta, ASAP
14. Gao Z-Y, Liu J-L, Chang J-L, Wu D-P, He J-L, Wang K, Xu F, Jiang K (2012) Mesocrystalline Cu_2O hollow nanocubes: synthesis and application in non-enzymatic amperometric detection of hydrogen peroxide and glucose. CrystEngComm 14:6639
15. Zhou D-L, Feng J-J, Cai L-Y, Fang Q-X, Chen J-R, Wang A-J (2014) Facile synthesis of monodisperse porous Cu_2O nanospheres on reduced graphene oxide for non-enzymatic amperometric glucose sensing. Electrochim Acta 115:103
16. You H, Yang S, Ding B, Yang H (2013) Synthesis of colloidal metal and metal alloy nanoparticles for electrochemical energy applications. Chem Soc Rev 42:2880

17. Zhang H, Jin M, Xia Y (2012) Noble-metal nanocrystals with concave surfaces: synthesis and applications. Angew Chem Int Ed 51:7656
18. Wang Y, Choi SI, Zhao X, Xie S, Peng HC, Chi M, Huang CZ, Xia Y (2014) Polyol synthesis of ultrathin Pd nanowires via attachment-based growth and their enhanced activity towards formic acid oxidation. Adv Funct Mater 24:131
19. Zhao D, Huo Q, Feng J, Chmelka BF, Stucky GD (1998) Nonionic triblock and star diblock copolymer and oligomeric surfactant syntheses of highly ordered, hydrothermally stable, mesoporous silica structures. J Am Chem Soc 120:6024
20. Zhao D, Feng J, Huo Q, Melosh N, Fredrickson GH, Chmelka BF, Stucky GD (1998) Triblock copolymer syntheses of mesoporous silica with periodic 50 to 300 angstrom pores. Science 279:548
21. Guo Y-Q, Sun X-Y, Liu Y, Wang W, Qiu H-X, Gao J-P (2012) One pot preparation of reduced graphene oxide (RGO) or Au (Ag) nanoparticle-RGO hybrids using chitosan as a reducing and stabilizing agent and their use in methanol electrooxidation. Carbon 50: 2513
22. Liu M-M, Liu R, Chen W (2013) Graphene wrapped Cu_2O nanocubes: non-enzymatic electrochemical sensors for the detection of glucose and hydrogen peroxide with enhanced stability. Biosens Bioelectron 45:206
23. Li B-J, Cao H-Q, Yin G, Lu Y-X, Yin J-F (2011) Cu_2O @ reduced graphene oxide composite for removal of contaminants from water and supercapacitors. J Mater Chem 21:10645
24. Gao Y-J, Ma D, Wang C-L, Guan J, Bao X-H (2011) Reduced graphene oxide as a catalyst for hydrogenation of nitrobenzene at room temperature. Chem Commun 47:2432
25. Paolella A, Brescia R, Prato M, Povia M, Marras S, De Trizio L, Falqui A, Manna L, George C (2013) Colloidal synthesis of cuprite (Cu_2O) octahedral nanocrystals and their electrochemical lithiation. ACS Appl Mater Interfaces 5:2745
26. Cochell T, Manthiram A (2012) Pt@Pd_xCu_y/C core–shell electrocatalysts for oxygen reduction reaction in fuel cells. Langmuir 28:1579
27. Wang C, Wang C-X, Xu L, Cheng H, Lin Q, Zhang C (2014) Protein-directed synthesis of pH-responsive red fluorescent copper nanoclusters and their applications in cellular imaging and catalysis. Nanoscale 6:1775
28. Li Y-J, Gao W, Ci L-J, Wang C-M, Ajayan PM (2010) Catalytic performance of Pt nanoparticles on reduced graphene oxide for methanol electro-oxidation. Carbon 48:1124
29. Lv J-J, Li S-S, Wang A-J, Mei L-P, Chen J-R, Feng J-J (2014) Monodisperse Au-Pd bimetallic alloyed nanoparticles supported on reduced graphene oxide with enhanced electrocatalytic activity towards oxygen reduction reaction. Electrochim Acta 136:521
30. Lv J-J, Feng J-X, Li S-S, Wang Y-Y, Wang A-J, Zhang Q-L, Chen J-R, Feng J-J (2014) Ionic liquid crystal-assisted synthesis of PtAg nanoflowers on reduced graphene oxide and their enhanced electrocatalytic activity toward oxygen reduction reaction. Electrochim Acta 133:407
31. Qiu J-D, Wang G-C, Liang R-P, Xia X-H, Yu H-W (2011) Controllable deposition of platinum nanoparticles on graphene as an electrocatalyst for direct methanol fuel cells. J Phys Chem C 115:15639
32. Meher SK, Cargnello M, Troiani H, Montini T, Rao GR, Fornasiero P (2013) Alcohol induced ultra-fine dispersion of pt on tuned morphologies of CeO_2 for CO oxidation. Appl Catal B 130:121
33. Luo J, Jiang S-S, Zhang H-Y, Jiang J-Q, Liu X-Y (2012) A novel non-enzymatic glucose sensor based on Cu nanoparticle modified graphene sheets electrode. Anal Chim Acta 709:47
34. Wang G-F, Wei Y, Zhang W, Zhang X, Fang B, Wang L (2010) Enzyme-free amperometric sensing of glucose using Cu-CuO nanowire composites. Microchim Acta 168:87
35. Wang A-J, Feng J-J, Li Z-H, Liao Q-C, Wang Z-Z, Chen J-R (2012) Solvothermal synthesis of Cu/Cu_2O hollow microspheres for non-enzymatic amperometric glucose sensing. CrystEngComm 14:1289
36. Fu S, Fan G, Yang L, Li F (2015) Non-enzymatic glucose sensor based on au nanoparticles decorated ternary Ni-Al layered double hydroxide/single-walled carbon nanotubes/graphene nanocomposite. Electrochim Acta 152:146
37. Li M, Liu L, Xiong Y, Liu X, Nsabimana A, Bo X, Guo L (2015) Bimetallic mco (M = Cu, Fe, Ni, and Mn) nanoparticles doped-carbon nanofibers synthetized by electrospinning for nonenzymatic glucose detection. Sens Actuators B 207:61